


Skyrmion Spin Ice in Liquid Crystals

 Ayhan Duzgun¹ and Cristiano Nisoli^{1*}
Theoretical Division, Los Alamos National Laboratory, Los Alamos, New Mexico 87545, USA
 (Received 21 October 2019; revised 17 October 2020; accepted 23 December 2020; published 26 January 2021)

We propose the first skyrmion spin ice, realized via confined, interacting liquid crystal skyrmions. Skyrmions in a chiral nematic liquid crystal behave as quasiparticles that can be dynamically confined, bound, and created or annihilated individually with ease and precision. We show that these quasiparticles can be employed to realize binary variables that interact to form ice-rule states. Because of their unique versatility, liquid crystal skyrmions can open entirely novel avenues in the field of frustrated systems. More broadly, our findings also demonstrate the viability of liquid crystal skyrmions as elementary degrees of freedom in the design of collective complex behaviors.

DOI: 10.1103/PhysRevLett.126.047801

Artificial spin ices (ASIs) [1–10] are frustrated materials modeled as arrays of interacting, frustrated, binary variables arranged along the edges of a lattice. At the vertices, where these Ising spins meet, their configurations obey the ice rule [11,12], which often leads to various forms of constrained disorder. ASIs can be designed for a wide variety of unusual emergent behaviors [10] often not found in natural materials [13,14]. Their seminal [1,2] and, to this day, most explored [8–10] realizations employ lithographically fabricated, magnetic nanoislands. Nonetheless, the same set of ideas behind these materials extend beyond magnetism, and spin ice physics has been exported to other platforms, such as superconductors [5–7,15], confined colloids [4,16,17], magnetic skyrmions [18], and elastic metamaterials [19].

In this Letter, we numerically demonstrate liquid crystals (LCs) as a new, timely platform for spin ice physics [20]. By confining liquid crystal skyrmions in binary traps with two preferential positions at the ends [3], we recreate Ising spin variables. Then, their frustrated mutual repulsion leads to the ice rule [3,21].

Nematic LCs are typically made of elongated molecules which can access phases of orientational order but no spatial order. They exhibit a random distribution of their centers of masses yet with the alignment of their principal axis along a local director $\hat{n}(\vec{x})$. Their nematicity can be captured by a traceless tensor $Q_{\alpha\beta} = S(3\hat{n}_\alpha\hat{n}_\beta - \delta_{\alpha\beta})/2$, S being the so-called scalar order parameter quantifying orientational order.

Our LC cell [Fig. 1(a)] consists of a chiral nematic LC confined between two parallel surfaces. The system is successfully described via a phenomenological free energy per unit volume

$$\begin{aligned}
 f = & \frac{1}{2}a\text{Tr}(Q^2) + \frac{1}{3}b\text{Tr}(Q^3) + \frac{1}{4}c[\text{Tr}(Q^2)]^2 \\
 & + \frac{1}{2}L(\partial_\gamma Q_{\alpha\beta})(\partial_\gamma Q_{\alpha\beta}) - \frac{4\pi}{p}L\epsilon_{\alpha\beta\gamma}Q_{\alpha\rho}\partial_\gamma Q_{\beta\rho} \\
 & - \{K[(\delta(z) + \delta(z - N_z)) + E^2\Delta\epsilon]Q_{zz}. \quad (1)
 \end{aligned}$$

The first line is the Landau-de Gennes [22,23] thermal term describing the nematic to isotropic second order phase transition in temperature [parameters a , b , and c are chosen to ensure a reasonable value for S , see Supplemental Material (SM) [24]]. In the second line, elastic energies (of single elastic constant L) penalize the gradient of Q and favor a twist with cholesteric pitch p . The last line reflects

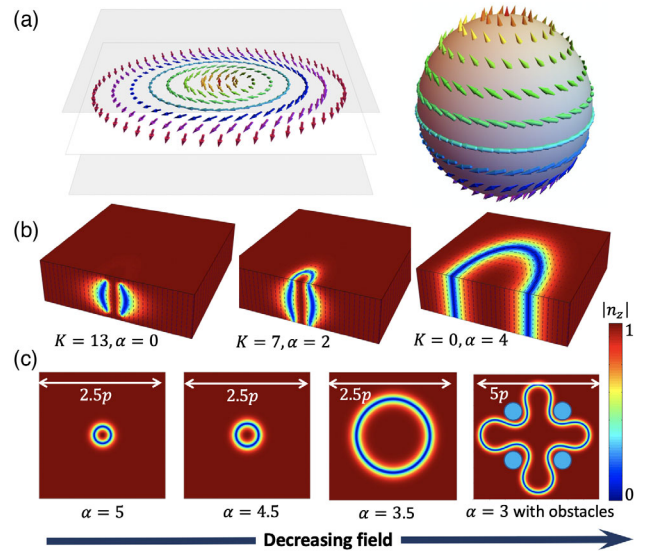


FIG. 1. Skyrmion structure. (a) Midlayer of a vectorized skyrmion in LC cell with homeotropic anchoring and mapping of directors on to the surface of a sphere. (b) External electric field (coupling coefficient α) and surface anchoring (coupling coefficient K) can be used in various proportions to sustain long lived skyrmions. Different skyrmion shapes appear depending on K and α . The ratio of the cell thickness to the cholesteric pitch is $N_z/p \approx 0.36$. (c) Top view of 2D skyrmions ($K = 0$) stabilized by background field (stability range $5.5 > \alpha > 3$ as shown in [25]). Reducing field strength results in increased skyrmion size and increased deformability near obstacles produced by strong vertical alignment (blue circles).

the homeotropic surface anchoring of strength K at the boundaries ($z = 0, N_z$) and the coupling to a uniform electric field E , applied in the z direction. $\Delta\epsilon$ is the dielectric anisotropy of the LC favoring easy-axis (along z) or easy-plane (perpendicular to z) alignment depending on its sign. We will express the coefficients of the alignment terms, K and $\alpha = \Delta\epsilon E^2$, in dimensionless units by setting $\alpha_0 = LSq_0^2 = 1$ and $K_0 = LSq_0 = 1$ where q_0 is the natural twist. Then, $K/K_0 = p/2\pi\xi_K$ and $\alpha/\alpha_0 = (p/2\pi\xi_E)^2$ where $\xi_K = LS/K$ is the anchoring extrapolation length and $\xi_E = \sqrt{LS/\alpha}$ is the electrostatic coherence length. Expressing Eq. (1) in dimensionless terms (see SM [24]) reveals that the ratios α/α_0 and $(K/K_0)/(N_z/p)$ determine the alignment strength.

Frustration in the form of alignment in the vertical direction can be used to stabilize particlelike solutions called skyrmions. Figure 1(a) shows the midplane of one such full skyrmion, where the polar angle of the director \vec{n} rotates by 180° from its center to periphery leading to a topological charge $(1/4\pi) \int \int dx dy \vec{n} \cdot (\partial_x \vec{n} \times \partial_y \vec{n}) = 1$, as the mapping of the directors to the surface of a sphere covers the surface once. In Fig. 1(b), we show skyrmions with the same topology whose size and shape are controlled by K and α , for a cell thickness $N_z = 0.36p$. When $K \neq 0$, skyrmions form barrel-like spherulites which can be fully embedded inside the cell. As K is further reduced and α becomes dominant, the z dependence becomes small, as also seen in experiments [26,27]. The special case of $K = 0$ yields a z -invariant structure [28,29], and can be modeled as 2D allowing the possibility of simulating very large systems. Finally, Fig. 1(c) demonstrates size control via the electric field which was previously studied in detail [25]. The main text includes only 2D simulations, and full 3D simulations are presented in the SM [24].

Crucially, unlike merons [25,30–32], LC skyrmions are local objects (not accompanied by defects) that can be generated and decimated at will as long lived isolated particles—they neither disappear, nor spontaneously appear [28,33–35]. They can be actuated, and arranged to exhibit a variety of collective dynamics [36–38]. Skyrmions can be confined, and manipulated via light, electric fields, and surface chemistry [26,27,39–41]. They are attracted by regions of weak (and repelled by regions of strong) easy-axis alignment [28,42]. Also, skyrmions are repelled from regions exposed to light, which increases the helical pitch p [43]. Finally, confinement by electrical field is not made problematic by fringe effects or lack of sharp gradients in real systems, as we have shown [28,42].

To build a spin ice, we need to confine skyrmions in binary traps that can be considered pseudospins [17], using the mechanisms above. The task is nontrivial. Previous works on colloids [3,4] suggest a dumbbell-shaped confinement [Fig. 2(a)]. This choice would not work for skyrmions because traps with closed ends would suppress their mutual elastic interaction. The second panel of Fig. 2(a) shows how

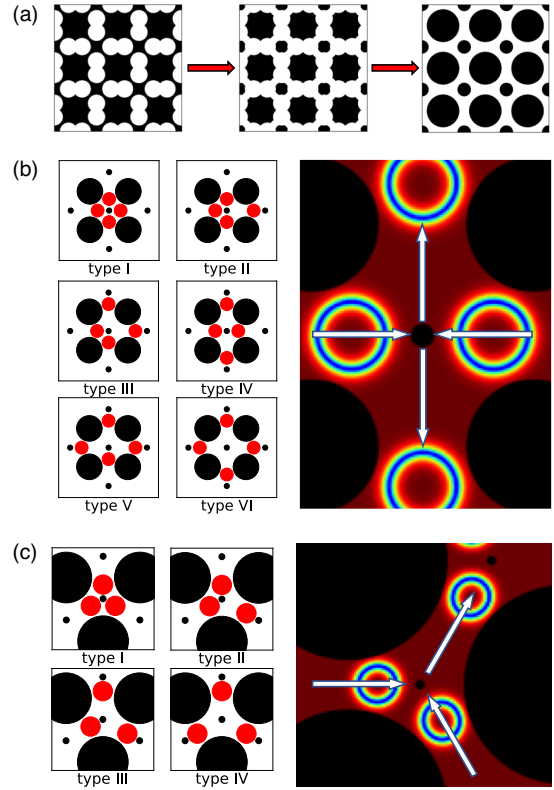


FIG. 2. Constructing binary variables out of trapped skyrmions. (a) Dumbbell traps with closed ends would suppress skyrmion-skyrmion interaction, hence, are modified to final design with open ends. (b) Schematics of vertex configuration types in order of decreasing energy for square skyrmionic ice. Red circles represent the skyrmions, and vertex types are listed in order of decreasing energy. Ice-rule configurations are the two type IV vertices corresponding to two skyrmions in the vertex, and two out of the vertex. (c) Vertex configurations in order of decreasing energy for hexagonal skyrmionic ice. Ice-rule configurations are the three type II vertices (two skyrmions in, one out) and three type III (one in, two out) vertices.

to go from dumbbells to our much simpler and general geometry with open ends. There, smaller black circles represent trap ends and bigger circles provide the narrower midsection of the trap.

The usual nomenclature [17] for skyrmions' configurations at the vertices is shown in Figs. 2(b) and 2(c) along with their spin representation for a square and hexagonal lattice, respectively. It is expected [3], as a result of nonlocal frustration [21], that collective lowest energy states obey the ice rule [11,12]: two particles in the vertex and two out for the square geometry and one in and two out for the hexagonal one. Further, the square geometry should lead to an ordered state and the hexagonal to a disordered one.

We run simulations of the LC systems of 2D skyrmions by solving the over-damped dynamic equation $\partial_t Q(\mathbf{r}, t) = -\Gamma \delta F / \delta Q(\mathbf{r}, t)$ [where $F = \int f(\mathbf{r}) d^3 r$ and Γ is the mobility constant] using a finite differences method and with

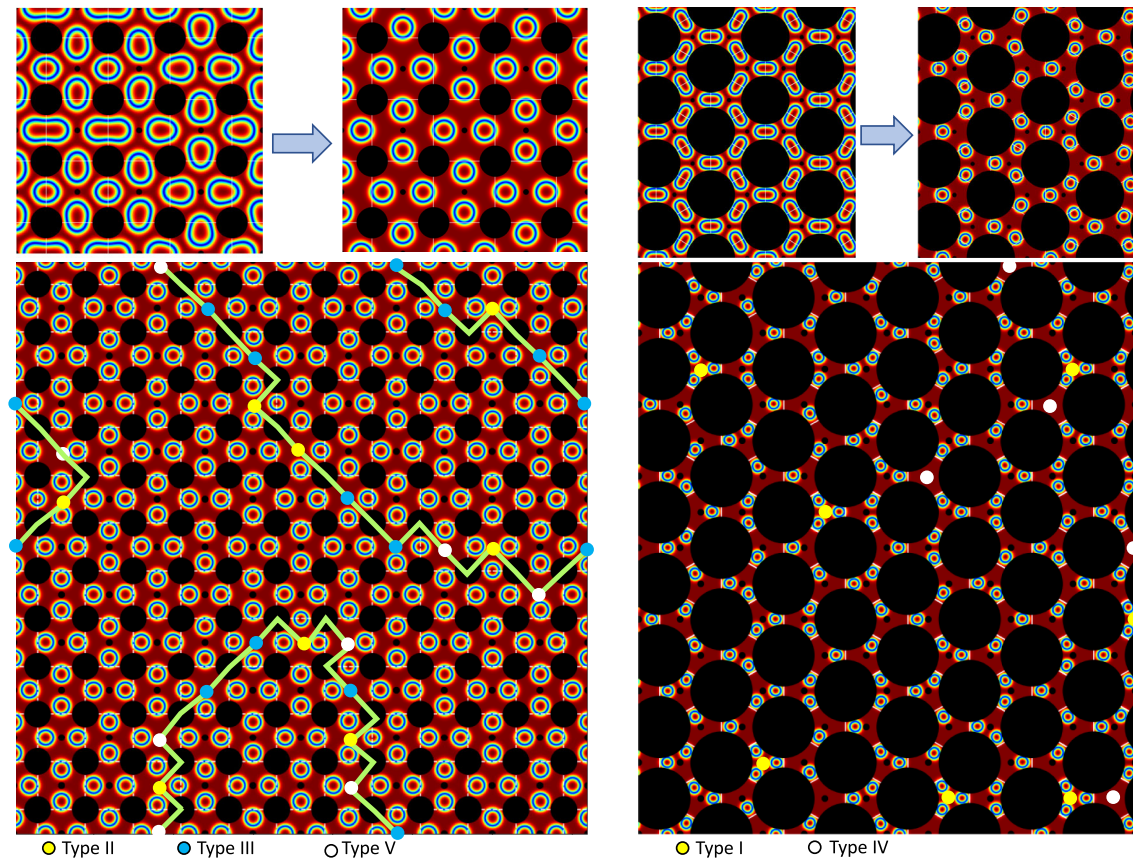


FIG. 3. Relaxed skyrmion spin ices obey the ice rule. Top: Skyrmions initially swollen and then deswollen, relax to lower energy states. Bottom: 2D square and hexagonal ice with surface anchoring or field relax to ice-rule-obeying states with defects. The square geometry shows an ordered state where domains of different “antiferromagnetic” orientations of ice rule, type IV vertices are separated by domain walls (green lines) of ice-rule-obeying type III (blue) and ice-rule-violating type II (yellow) and type V (white). The hexagonal geometry converges to a disordered manifold of ice-rule-obeying type II (two in and one out) and type III (one in and two out) vertices. Excitations are ice-rule-violating type I (three in, yellow) or type IV (three out, white) vertices. White lines superimposed on the lattices highlight the midpoint of the traps. Aspect ratios of the traps are 0.52 for square and 0.41 for hexagonal lattices. Other simulation parameters are listed in the Supplemental Material [24].

periodic boundary conditions [25,28,42]. Traps are realized via either extra field or surface anchoring. We initiate the system in an unrelaxed state with 288 skyrmions in the square geometry and 192 in the hexagonal geometry placed randomly inside the traps. This entails about 3×10^6 elements updated at each time step, which we implement by exploiting the intrinsic parallelism of graphics processing units (see SM [24]). Systems were updated for 10^7 time steps for the square and 3×10^7 time steps for the hexagonal lattice. At the beginning, we reduce the background field to swell the skyrmions until they occupy almost their entire traps (Fig. 3, top and SM [24]) so as to bring them in close interaction, and then we deswell the skyrmions and let the system relax.

Figure 3 shows snapshots of the final states for the two geometries. Square ice converges to an ordered antiferromagnetic [3,44,45] tessellation of ice-rule-obeying type IV vertices, with two skyrmions close to, and two away from, each vertex. Deviations from type IV correspond

to ice-rule-obeying type III, but also to violations of the ice rule in the form of monopoles [46], or type II and type V. Together, these excitations form familiar domain walls (drawn according to the method in Ref. [47]) among the two possible orientations of antiferromagnetic order. Hexagonal ice also converges properly to an ice state where, unlike square ice, a disordered mixture of type II and type III obey the (pseudo)ice rule (one in and two out and two in and one out), together with sparse monopole defects (types I, IV).

Structural parameters control proximity to the ice rule. Consider the aspect ratio of traps ω/D , where ω is the width of the middle of the trap and D is the length of the edge of the lattice. If ω/D is too small [pink region in Figs. 4(a) and 4(b)], the skyrmions are frozen in the trap; if too large (violet region), the trap is no longer binary and the skyrmions can sit at the center. The transition to this second regime is interesting, as it can lead to the realization of a still largely unexplored classical spin-1 ice model where

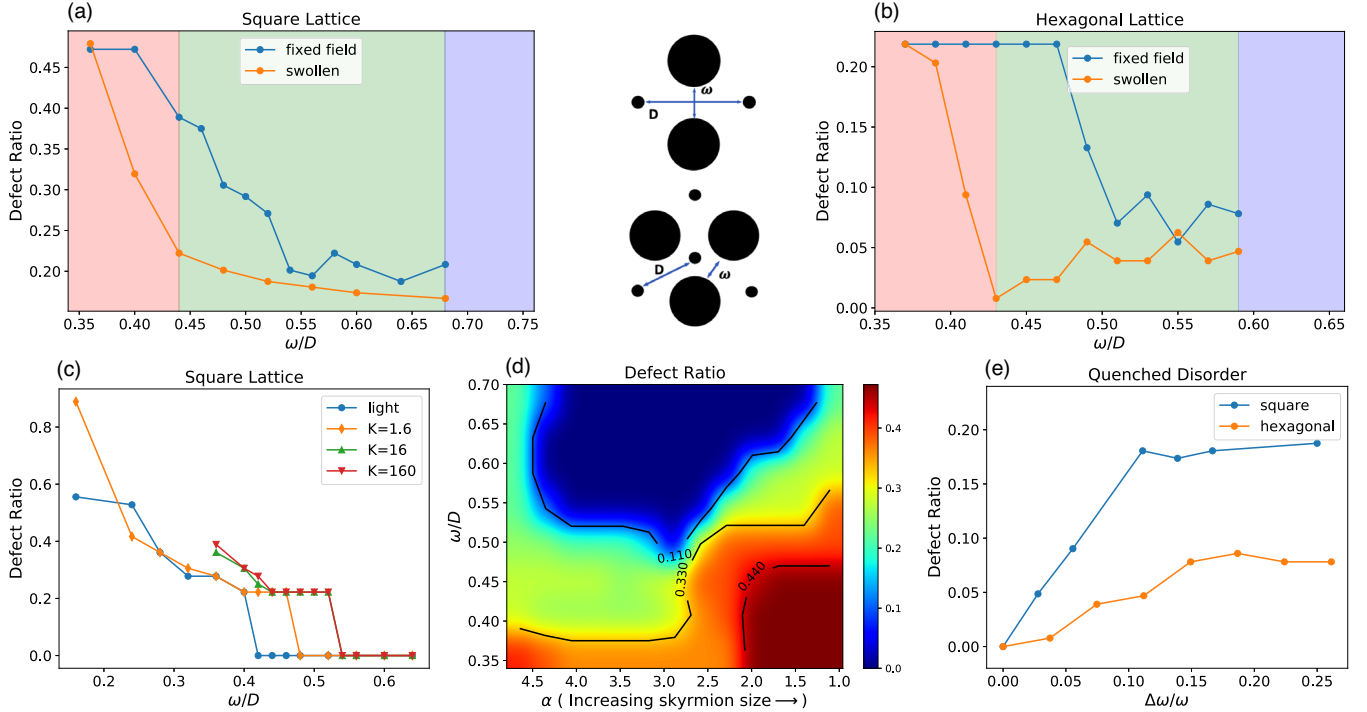


FIG. 4. Limits of the ice-rule validity. (a),(b) Defect ratio vs size of the central circle in the trap for square and hexagonal lattices. Purple region: ω values too large for trap asymmetry. Pink region: ω values too small to allow skyrmion motion. Green region: ice behavior observed. (c) Suitable obstacle size depends on the type of wall mechanism and its strength. Results for obstacles produced by light and by various strengths of surface anchoring K inside the obstacles are shown. (d) Skyrmion size also influences how traps work. Ice rule is not observed for very large or very small skyrmions. (e) Defect counts vs random noise added to the width of traps. The noise is uniformly distributed between $\pm\Delta\omega$ with $D = 60$ and $\omega/D = 0.6$. Other simulation parameters are listed in the Supplemental Material [24].

spins can be $-1, 0, 1$, and will be explored in future work. At intermediate values (green region), we are closest to the ice rule.

The distinction between the three regions is fuzzy, also, because the system preserves memory of its preparation. Figures 4(a) and 4(b) show that cyclically swelling and deswelling the skyrmions helps the system find lower energy states and extends the suitable range for ice configurations after two to three cycles and leads to states closer to the ice rule. More cycles do not change the final state. Figure 4(c) shows how curves of ice-rule violations vs aspect ratio for square ice vary depending on obstacle properties. Obstacles generated by weaker anchoring ($K = 1.6$) are softer and allow increased mobility for the skyrmions, thus, helping the system reach the ice state. Also, note that $K = 16$ and $K = 160$ have identical effects, indicating that the effect saturates rapidly in K . Light exposure was modeled by reducing $q_0 \rightarrow q_0/1.2$ and produces an effect similar to changing $K \rightarrow 1.2K$ as the relevant ratio is K/LSq_0 .

Another relevant structural parameter is skyrmion size. In a previous work [25], we found that unconfined skyrmions exist for $3 < \alpha < 5.5$ (smaller size at larger α). The confining effect of traps, however, allows for skyrmions to exist even for $\alpha = 0$. It becomes interesting, then, to study the combined

effect of trap aspect ratio and skyrmion size. Figure 4(d) shows a contour plot of the defect count vs ω/D and α demonstrating different regimes, including a blue area where defects are less than 10%. In agreement with Fig. 4(a), already discussed, the $\omega/D > 0.5$ region corresponds to minimal defects. There, we observe an ample blue region, where the ice configuration is reached easily and not affected much by the value of α . When skyrmions become too small ($\alpha > 4.5$), however, they do not interact, and we see more defects. On the opposite side, if skyrmions are too big compared with trap width they cannot properly move within the trap, and defects also increase. Therefore, the demarcating line among regimes is approximately linear.

Finally, previous spin ices are relatively robust against weak quenched disorder [48–50]. To test our proposal, we introduce disorder in the positions of the bigger circular walls while keeping the trap ends unchanged, leading to a random shift between $-\Delta\omega$ and $+\Delta\omega$. Figure 4(e) shows that disorder affects the square geometry more than the hexagonal. That is expected, as square spin ice has an ordered ground state and its excitations are strongly correlated via the domain walls of Fig. 3. Instead, sparse monopole defects in hexagonal spin ice are weakly correlated.

One last note. The reader will have noticed that the statistics of Figs. 4(c)–4(e) can reach zero defects whereas

Fig. 4(a) does not (intentionally chosen to illustrate connected unhappy vertices). The reason is that the system employed in Figs. 4(c) and 4(d) is four times smaller and, thus, can more easily reach low energy states. In Fig. 4(e), the system size is the same as in Fig. 4(a), but the simulation time is 4 times as long (parameters are shown in the Supplemental Material [24]).

We have numerically demonstrated LCs as a new platform for spin ice physics on the two most common geometries. In future works, we will explore extension to more complex geometries [14,51–53]. Unlike previous platforms, LCs can allow dynamic change of structure, for instance, for cycling between topologically equivalent geometries of different ice behavior, for memory effects. Unlike trapped colloids, the skyrmions can change size, can be created or destroyed optically on the fly, to explore decimation, ice-rule fragility [16], or doping [54]. Their mutual interaction can be controlled, from anisotropic to isotropic, by changing the direction of the background field [55,56]. A growing abundance of techniques for controlling the collective behavior of LC topological defects suggests employment for actuation in soft robotics, optical applications, and functional materials design. Our proposal to realize spin ice with LC skyrmions is a promising development in this direction, which we believe will stimulate experimental efforts.

We wish to thank Ivan Smalyukh and Hayley Sohn (University of Colorado at Boulder) for useful discussions on skyrmion confinement and manipulation and Michael Varga for discussions on CUDA programming. This work was carried out under the auspices of the U.S. Department of Energy through the Los Alamos National Laboratory, operated by Triad National Security, LLC (Contract No. 892333218NCA000001) and funded by DOE-LDRD.

*cristiano@lanl.gov; cristiano.nisoli.work@gmail.com

- [1] R. F. Wang, C. Nisoli, R. S. Freitas, J. Li, W. McConville, B. J. Cooley, M. S. Lund, N. Samarth, C. Leighton, V. H. Crespi, and P. Schiffer, Artificial ‘spin ice’ in a geometrically frustrated lattice of nanoscale ferromagnetic islands, *Nature (London)* **439**, 303 (2006).
- [2] M. Tanaka, E. Saitoh, H. Miyajima, T. Yamaoka, and Y. Iye, Magnetic interactions in a ferromagnetic honeycomb nanoscale network, *Phys. Rev. B* **73**, 052411 (2006).
- [3] A. Libál, C. Reichhardt, and C. J. O. Reichhardt, Realizing Colloidal Artificial Ice on Arrays of Optical Traps, *Phys. Rev. Lett.* **97**, 228302 (2006).
- [4] A. Ortiz-Ambriz and P. Tierno, Engineering of frustration in colloidal artificial ices realized on microfeatured grooved lattices, *Nat. Commun.* **7**, 10575 (2016).
- [5] A. Libál, C. J. O. Reichhardt, and C. Reichhardt, Creating Artificial Ice States Using Vortices in Nanostructured Superconductors, *Phys. Rev. Lett.* **102**, 237004 (2009).
- [6] M. L. Latimer, G. R. Berdiyrov, Z. L. Xiao, F. M. Peeters, and W. K. Kwok, Realization of Artificial Ice Systems for Magnetic Vortices in a Superconducting MoGe Thin Film with Patterned Nanostructures, *Phys. Rev. Lett.* **111**, 067001 (2013).
- [7] J. Trastoy, M. Malnou, C. Ulysse, R. Bernard, N. Bergeal, G. Faini, J. Lesueur, J. Briatico, and J. E. Villegas, Freezing and thawing of artificial ice by thermal switching of geometric frustration in magnetic flux lattices, *Nat. Nanotechnol.* **9**, 710 (2014).
- [8] C. Nisoli, R. Moessner, and P. Schiffer, Colloquium: Artificial spin ice: Designing and imaging magnetic frustration, *Rev. Mod. Phys.* **85**, 1473 (2013).
- [9] L. J. Heyderman and R. L. Stamps, Artificial ferroic systems: Novel functionality from structure, interactions and dynamics, *J. Phys. Condens. Matter* **25**, 363201 (2013).
- [10] C. Nisoli, Frustration(s) and the ice rule: From natural materials to the deliberate design of exotic behaviors, in *Frustrated Materials and Ferroic Glasses* (Springer, New York, 2018), pp. 57–99.
- [11] J. D. Bernal and R. H. Fowler, A theory of water and ionic solution, with particular reference to hydrogen and hydroxyl ions, *J. Chem. Phys.* **1**, 515 (1933).
- [12] L. Pauling, The structure and entropy of ice and of other crystals with some randomness of atomic arrangement, *J. Am. Chem. Soc.* **57**, 2680 (1935).
- [13] I. Gilbert, C. Nisoli, and P. Schiffer, Frustration by design, *Phys. Today* **69**, 7, 54 (2016).
- [14] C. Nisoli, V. Kapaklis, and P. Schiffer, Deliberate exotic magnetism via frustration and topology, *Nat. Phys.* **13**, 200 (2017).
- [15] Y.-L. Wang, X. Ma, J. Xu, Z.-L. Xiao, A. Snezhko, R. Divan, L. E. Ocola, J. E. Pearson, B. Janko, and W.-K. Kwok, Switchable geometric frustration in an artificial-spin-ice–superconductor heterosystem, *Nat. Nanotechnol.* **13**, 560 (2018).
- [16] A. Libál, D. Y. Lee, A. Ortiz-Ambriz, C. Reichhardt, C. J. O. Reichhardt, P. Tierno, and C. Nisoli, Ice rule fragility via topological charge transfer in artificial colloidal ice, *Nat. Commun.* **9**, 4146 (2018).
- [17] A. Ortiz-Ambriz, C. Nisoli, C. Reichhardt, C. J. O. Reichhardt, and P. Tierno, Colloquium: Ice rule and emergent frustration in particle ice and beyond, *Rev. Mod. Phys.* **91**, 041003 (2019).
- [18] F. Ma, C. Reichhardt, W. Gan, C. J. Olson Reichhardt, and W. S. Lew, Emergent geometric frustration of artificial magnetic skyrmion crystals, *Phys. Rev. B* **94**, 144405 (2016).
- [19] A. S. Meeussen, E. C. Oguz, Y. Shokef, and M. van Hecke, Topological defects produce exotic mechanics in complex metamaterials, *Nat. Phys.* **16**, 307 (2020).
- [20] A. Duzgun and C. Nisoli, Artificial spin (and potts) ice of skyrmions in liquid crystals, *APS March Meeting Abstracts* (2019), abs. ID C30.010, <http://meetings.aps.org/Meeting/MAR19/Session/C30.10>.
- [21] C. Nisoli, Unexpected Phenomenology in Particle-Based Ice Absent in Magnetic Spin Ice, *Phys. Rev. Lett.* **120**, 167205 (2018).
- [22] P. G. de Gennes and J. Prost, *The Physics of Liquid Crystals*, 2nd ed. (Clarendon Press, Oxford, 1993).
- [23] H. Grebel, R. M. Hornreich, and S. Shtrikman, Landau theory of cholesteric blue phases, *Phys. Rev. A* **28**, 1114 (1983).

- [24] See Supplemental Material at <http://link.aps.org/supplemental/10.1103/PhysRevLett.126.047801> for simulation methods and parameters, supplemental videos, a discussion on length scales in the system, and a discussion on obstacles generated by point electrodes.
- [25] A. Duzgun, J. V. Selinger, and A. Saxena, Comparing skyrmions and merons in chiral liquid crystals and magnets, *Phys. Rev. E* **97**, 062706 (2018).
- [26] P. J. Ackerman, R. P. Trivedi, B. Senyuk, J. van de Lagemaat, and I. I. Smalyukh, Two-dimensional skyrmions and other solitonic structures in confinement-frustrated chiral nematics, *Phys. Rev. E* **90**, 012505 (2014).
- [27] J.-S. B. Tai and I. I. Smalyukh, Surface anchoring as a control parameter for stabilizing torons, skyrmions, twisted walls, fingers, and their hybrids in chiral nematics, *Phys. Rev. E* **101**, 042702 (2020).
- [28] A. Duzgun, A. Saxena, and J. V. Selinger, Alignment induced reconfigurable walls for patterning and assembly of liquid crystal skyrmions, *Phys. Rev. Research* **3**, L012005 (2021).
- [29] G. De Matteis, L. Martina, and V. Turco, Skyrmion states in chiral liquid crystals, *Theor. Math. Phys.* **196**, 1150 (2018).
- [30] J.-i. Fukuda and S. Zumer, Quasi-two-dimensional skyrmion lattices in a chiral nematic liquid crystal, *Nat. Commun.* **2**, 246 (2011).
- [31] A. Nych, J.-i. Fukuda, U. Ognysta, S. Zumer, and I. Musevic, Spontaneous formation and dynamics of half-skyrmions in a chiral liquid-crystal film, *Nat. Phys.* **13**, 1215 (2017).
- [32] L. Metselaar, A. Doostmohammadi, and J. M. Yeomans, Topological states in chiral active matter: Dynamic blue phases and active half-skyrmions, *J. Chem. Phys.* **150**, 064909 (2019).
- [33] D. Foster, C. Kind, P. J. Ackerman, J.-S. B. Tai, M. R. Dennis, and I. I. Smalyukh, Two-dimensional skyrmion bags in liquid crystals and ferromagnets, *Nat. Phys.* **15**, 655 (2019).
- [34] B. Berteloot, I. Nys, G. Poy, J. Beeckman, and K. Neyts, Ring-shaped liquid crystal structures through patterned planar photo-alignment, *Soft Matter* **16**, 4999 (2020).
- [35] O. D. Lavrentovich, Design of nematic liquid crystals to control microscale dynamics, [arXiv:2007.02187](https://arxiv.org/abs/2007.02187).
- [36] H. R. O. Sohn, C. D. Liu, Y. Wang, and I. I. Smalyukh, Light-controlled skyrmions and torons as reconfigurable particles, *Opt. Express* **27**, 29055 (2019).
- [37] P. J. Ackerman, T. Boyle, and I. I. Smalyukh, Squirming motion of baby skyrmions in nematic fluids, *Nat. Commun.* **8**, 673 (2017).
- [38] H. R. O. Sohn, P. J. Ackerman, T. J. Boyle, G. H. Sheetah, B. Fornberg, and I. I. Smalyukh, Dynamics of topological solitons, knotted streamlines, and transport of cargo in liquid crystals, *Phys. Rev. E* **97**, 052701 (2018).
- [39] Y. Guo, S. Afghah, J. Xiang, O. D. Lavrentovich, R. L. B. Selinger, and Q.-H. Wei, Cholesteric liquid crystals in rectangular microchannels: Skyrmions and stripes, *Soft Matter* **12**, 6312 (2016).
- [40] Y. H. Kim, M.-J. Gim, H.-T. Jung, and D. K. Yoon, Periodic arrays of liquid crystalline torons in microchannels, *RSC Adv.* **5**, 19279 (2015).
- [41] L. Cattaneo, Z. Kos, M. Savoini, P. Kouwer, A. Rowan, M. Ravnik, I. Musevic, and T. Rasing, Electric field generation of skyrmion-like structures in a nematic liquid crystal, *Soft Matter* **12**, 853 (2016).
- [42] A. Duzgun, C. Nisoli, C. Reichhardt, and C. Reichhardt, Commensurate states and pattern switching via liquid crystal skyrmions trapped in a square lattice, *Soft Matter* **16**, 3338 (2020).
- [43] H. Sohn, P. Ackerman, and I. Smalyukh, Optical patterning and dynamics of torons and hopfions in a chiral nematic with photo-tunable equilibrium pitch, *APS March Meeting Abstracts* (2017), abs. ID A17.013, <http://meetings.aps.org/Meeting/MAR17/Event/287743>.
- [44] S. Zhang, I. Gilbert, C. Nisoli, G.-W. Chern, M. J. Erickson, L. O'Brien, C. Leighton, P. E. Lammert, V. H. Crespi, and P. Schiffer, Crystallites of magnetic charges in artificial spin ice, *Nature (London)* **500**, 553 (2013).
- [45] J. M. Porro, A. Bedoya-Pinto, A. Berger, and P. Vavassori, Exploring thermally induced states in square artificial spin-ice arrays, *New J. Phys.* **15**, 055012 (2013).
- [46] C. Castelnovo, R. Moessner, and S. L. Sondhi, Magnetic monopoles in spin ice, *Nature (London)* **451**, 42 (2008).
- [47] C. Nisoli, Topological order in the six-vertex antiferromagnet and its breakdown in spin ice, [arXiv:2004.02107](https://arxiv.org/abs/2004.02107).
- [48] Z. Budrikis, J. P. Morgan, J. Akerman, A. Stein, P. Politi, S. Langridge, C. H. Marrows, and R. L. Stamps, Disorder Strength and Field-Driven Ground State Domain Formation in Artificial Spin Ice: Experiment, Simulation, and Theory, *Phys. Rev. Lett.* **109**, 037203 (2012).
- [49] Z. Budrikis, P. Politi, and R. L. Stamps, Diversity Enabling Equilibration: Disorder and the Ground State in Artificial Spin Ice, *Phys. Rev. Lett.* **107**, 217204 (2011).
- [50] Z. Budrikis, P. Politi, and R. L. Stamps, Disorder regimes and equivalence of disorder types in artificial spin ice, *J. Appl. Phys.* **111**, 07E109 (2012).
- [51] M. J. Morrison, T. R. Nelson, and C. Nisoli, Unhappy vertices in artificial spin ice: New degeneracies from vertex frustration, *New J. Phys.* **15**, 045009 (2013).
- [52] Y. Lao, F. Caravelli, M. Sheikh, J. Sklenar, D. Gardezabal, J. D. Watts, A. M. Albrecht, A. Scholl, K. Dahmen, C. Nisoli *et al.*, Classical topological order in the kinetics of artificial spin ice, *Nat. Phys.* **14**, 723 (2018).
- [53] A. Farhan, C. F. Petersen, S. Dhuey, L. Anghinolfi, Q. Hang Qin, M. Saccone, S. Velten, C. Wuth, S. Gliga, P. Mellado *et al.*, Nanoscale control of competing interactions and geometrical frustration in a dipolar trident lattice, *Nat. Commun.* **8**, 995 (2017).
- [54] A. Libál, C. J. Olson Reichhardt, and C. Reichhardt, Doped colloidal artificial spin ice, *New J. Phys.* **17**, 103010 (2015).
- [55] A. Saxena and A. Duzgun, Interaction of liquid crystal skyrmions with curved boundaries, *APS March Meeting Abstracts* (2019), abs. ID B30.011, <https://meetings.aps.org/Meeting/MAR19/Session/B30.11>.
- [56] H. R. O. Sohn, C. D. Liu, and I. I. Smalyukh, Schools of skyrmions with electrically tunable elastic interactions, *Nat. Commun.* **10**, 4744 (2019).